Raman mapping probing of tip-induced anomalous polarization behavior in V_2O_5 waveguiding nanoribbons

Bin Yan,[1] Chaoling Du,[1] Lei Liao,[1] Yumeng You,[1] Hao Cheng,[2] Zexiang Shen,[1] and Ting Yu[1,a)]

[1]*Division of Physics and Applied Physics, School of Physical and Mathematical Sciences, Nanyang Technological University, Singapore 637371, Singapore*

[2]*Division of Materials Technology, School of Materials Science and Engineering, Nanyang Technological University, Singapore 639798, Singapore*

(Received 31 October 2009; accepted 19 January 2010; published online 16 February 2010)

Spatially resolved and polarized micro-Raman spectroscopy has been performed on individual V_2O_5 waveguiding nanoribbons. The experimental results establish that the Raman-antenna patterns are strongly correlated with the *local* positions of the sample, which gives rise to a pronounced intensity contrast in the polarized mapping for certain phonon modes. The suppressed phonon signals at the body of a ribbon can be enhanced at the end facets, resulting from the effective waveguiding propagation along the nanoribbon and strong local electric field intensity at the ends. The phenomena reported here, in addition to providing insight into the tip effects on optoelectronic nanodevices, will facilitate the rational design of Raman detection in nanostructures. © *2010 American Institute of Physics*. [doi:10.1063/1.3323090]

One-dimensional (1D) nanostructure is expected to be a critical component in future optoelectronic devices and represents a unique system for exploring phenomena at the nanoscale.[1,2] Recently, significant progress has shown that the optical properties of the 1D specimen exhibit strong polarization anisotropy, due to the dielectric constant mismatch between a nanowire and its surroundings.[3,4] However, most of the work focuses only on the spectra from the body of nanowire, which assumed the nanowire as a circular dielectric cylinder of infinite length.[4–6] Nevertheless, nanowire tips have different boundary conditions from the body, thus are expected to affect the optical spectra. In this context, it is crucial to describe effects at the nanowire tips, which have been shown to play important roles in nanolasing resonators to confine photons and tip-enhanced Raman scattering, etc.[7,8] Therefore, spatially resolved imaging of a single nanostructure, which can provide detailed information on the localized area of interest, is particularly significant. Micro-confocal polarized Raman mapping is a promising technique for probing the physical properties of individual nanostructures in the rapidly evolving area of nanoscience with a reasonable spatial resolution.[9,10] In this letter, we report the use of polarized Raman imaging technique as a local characterization tool of an individual V_2O_5 nanoribbon. The exquisite spatial sensitivity allows for the distinction between different optical properties at the ends and body of the sample. It is found that the natural dependence of Raman tensors and the strong polarized local field can lead to two distinct types of Raman-antenna patterns at the body and tips of one-dimension nanostructures.

The experimental details can be founded in the supplemental information.[11] Polarized Raman images on individual nanoribbon, constructed by extracting integrated intensities of different phonon modes (A_g:996 cm^{-1}; B_{1g}:702 cm^{-1}; and B_{2g}:143 cm^{-1}), are shown in Fig. 1(a) by recording the data with about 200 nm/pixel and an integration time of 0.5 s/pixel. Considering the polarization dependences, two distinct homogeneous contrast images of A_g modes for different polarization geometries demonstrate the high crystalline quality along the nanoribbon,[10] which is also consistent with our TEM result.[11] Meanwhile, one of the most dramatic phenomena is that, B_{1g} (B_{2g}) modes exhibit predominant emission at the tips in $Z(XX)\bar{Z}$ configuration in contrast to the uniform intensity distribution along the nanoribbon for $Z(XY)\bar{Z}$ geometry and show a strong polarization dependence. In other words, B_{1g} and B_{2g} can be notably enhanced at end facets of the nanoribbon in $Z(XX)\bar{Z}$ configuration. Ac-

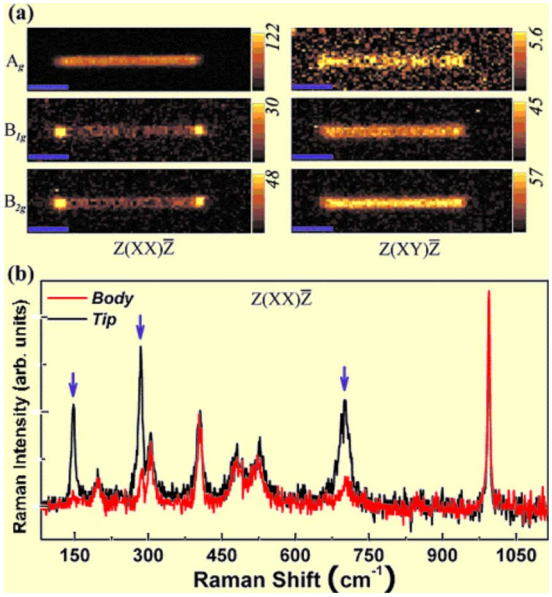

FIG. 1. (Color online) (a) Raman images of the nanoribbon constructed by extracting the integrated intensities of the different modes for $Z(XX)\bar{Z}$ and $Z(XY)\bar{Z}$ polarization configurations. The scale bar is 5 μm. (b) Raman scattering signals at the body and tip of sample under $Z(XX)\bar{Z}$ configuration.

a)Author to whom correspondence should be addressed. Electronic mail: yuting@ntu.edu.sg.

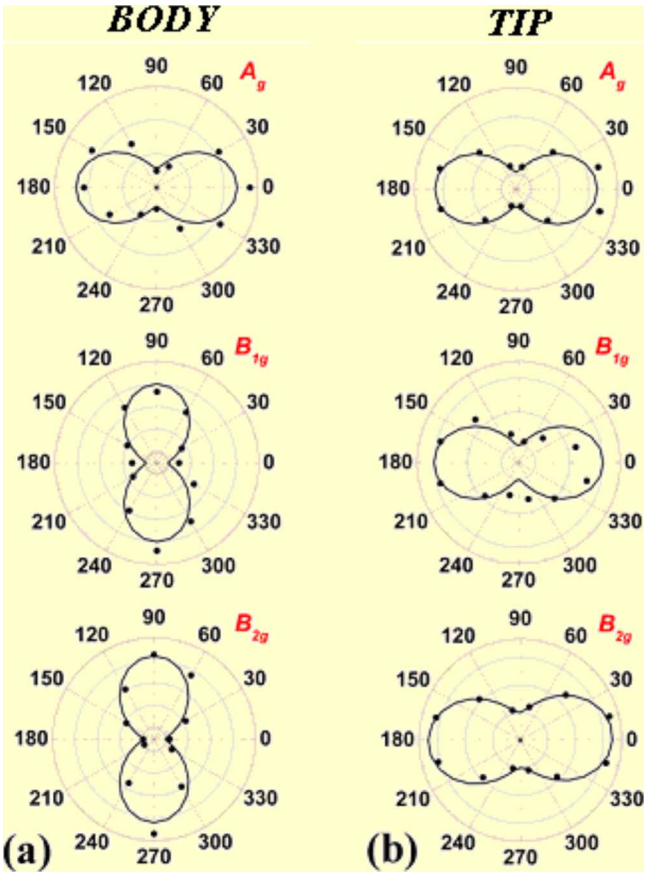

FIG. 2. (Color online) Polar plots for A_g, B_{1g}, and B_{2g} scattering intensities vs polarization angle θ, from the body (a) and tip (b) of the nanoribbon, respectively.

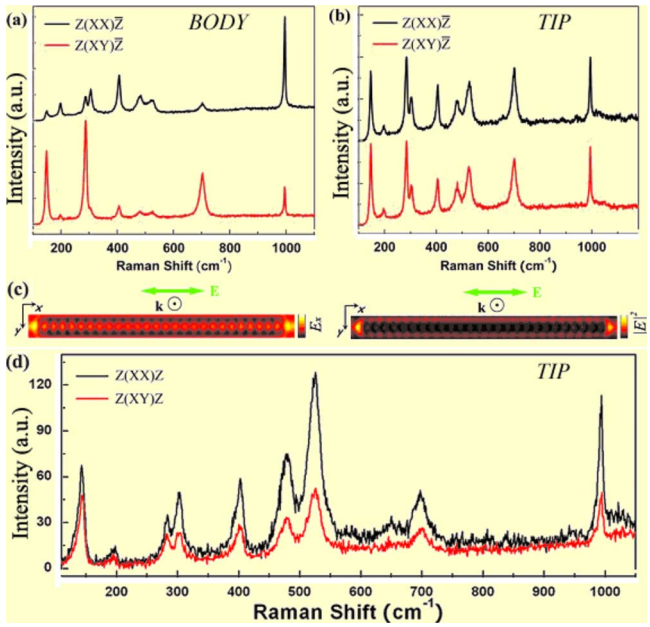

FIG. 3. (Color online) Comparison of the normalized polarized Raman spectra parallel $(Z(XX)\bar{Z})$ and orthogonal $(Z(XY)\bar{Z})$ to the nanoribbon axis collected at the body (a) and tip (b) of sample. (c) The simulated field distribution of a V_2O_5 nanoribbon (400 nm×250 nm×15 μm). (d) Waveguided Raman spectra out-coupled at the tip of the nanoribbon under parallel $(Z(XX)Z)$ and perpendicular $(Z(XY)Z)$ polarized collection conditions, respectively.

tually, as shown in Fig. 1(b), no obvious intensity change was observed on A_g modes, while pronounced B_{1g} and B_{2g} emission from the tips can be collected (which are labeled with arrows). Understanding of these results, in addition to providing insight into geometry-broken induced optical properties, will facilitate the rational design of Raman detection in nanostrutures.

To further explore the origin of the phenomenon described above, we have compared the angular dependence of the Raman emission from body and tip of the V_2O_5 nanoribbon which shows striking differences.[11] Note that the unique rectangle cross-section provides the complete orientation of the crystal axes relative to the plane of the substrate. So the polarization dependence of different phonon modes can be predicted accurately based on the Raman tensor analysis.[11] As shown in Fig. 2(a), the polarization dependent intensities from the body of nanoribbon are, in general, consistent with the Raman tensor analysis. Therefore, the antenna effects on the body of nanoribbon should have nothing to do with the phonon confinement. All the A_g modes have the maximum at θ=0°, which corresponds to the $Z(XX)\bar{Z}$ configuration, while both B_{1g} and B_{2g} modes follow the square of sine function and get maximum at θ=90°, equivalent to the $Z(XY)\bar{Z}$ configuration. This feature was further confirmed by the polarized Raman spectra from the body of sample [Fig. 3(a)], which shows a strong anisotropic behavior. The Raman intensity is normalized to the maximum intensity. Also, the relative intensity for B_{1g} (B_{2g}) modes in $Z(XY)\bar{Z}$ configuration became predominant compared to that in $Z(XX)\bar{Z}$ configuration. In contrast, when we focus the laser at the tips of nanoribbons, the spectra under different experimental setup exhibit similar line shapes as shown in Fig. 3(b). *Furthermore*, we surprisingly found that in our case all the phonon modes detected at the tip exhibit the same dipole-antenna polarization behavior which can be well-described by a $\cos^2\theta$ function [Fig. 2(b)]. Actually, in $Z(XX)\bar{Z}$ configuration (θ=0°, corresponding to the nanoribbon axis parallel to the direction of the analyzer) the B_{1g} and B_{2g} modes are suppressed at the body of sample while enhanced at the ends. Meanwhile, A_g modes do not show much suppression either at the tip or body of nanoribbon. Thus, we can expect that the appearance of the bright spots at both tips for B_{1g}- and B_{2g}-mode peaks, while homogenous spatial distribution of the A_g emission along the ribbon (as shown in Fig. 1).

The polarization anisotropy is very useful for the selective detection of certain phonons. Fréchette and Carraro[12] have reported that the large suppression of the depolarized signal provides an opportunity to increase the sensitivity of Raman scattering from surface modes relative to bulk modes. In our case, the results show that the sensitivity of Raman modes could also be changed due to the local positions. At the tip of nanoribbon, a different boundary condition could be expected compared to the middle portion. Recently, Poborchii[13] also reported that the edge brings about a strong electric field with a resultant Raman signal enhancement. Combined with the anisotropy of the dielectric susceptibility tensor, the different electric field components could result into a change of in/out-coupling efficiency. The local electric field intensities along the nanoribbon were simulated by finite element method, as shown in Fig. 3(c). Light (532 nm) was taken to be incident normal to the nanoribbon axis and electric field was parallel to the nanoribbon axis (transverse magnetic polarization). It can be seen that the calculated

electric field intensity has "hotspots" at the tips of the nanoribbon. Under these circumstances, it is conceivable that the outcoupling is strongly enhanced at the tips of sample, which would be directly related to the direction of the polarization of the scattering light.[6,14] Hence, the suppressed phonon signals at the body of a ribbon intensifying at the end facets could be expected. The results also indicate the potential applications for polarized tip-emission light source.[15]

In addition, the squared cosine dependency [as shown in Fig. 2(b)] can be rationalized by considering the effective waveguiding propagation along the nanoribbon of the nanostructure and the strong local intensity at the end of the nanostructures.[8,13,16] The propagation of Raman signals along V_2O_5 nanoribbon has been reported.[2] In the present case, the suppressed Raman signals can be guided along the nanoribbon to exit at the tip and result into a strong polarized outcoupling emission (enhanced parallel to the nanoribbon axis and suppressed perpendicular to the nanoribbon axis). To demonstrate the optical propagation effect on V_2O_5 nanoribbons, we have explored the spectral variation of polarized Raman-active waveguide emission using a WITEC CRM200 Raman system.[11] It is apparent from the spectra shown in Fig. 3(d) that intensities of all the Raman modes were significantly decreased when the collection polarizer was oriented perpendicular to the long axis of the nanoribbon, consistent with the polar plots in Fig. 2(b). By the detailed analysis of the polarization dependence of the emission, the waveguide-assisted nature of the Raman scattering has been proven. Several nanoribbons with different cross-sections were also tested. It was found that polarization anisotropy exhibits strong dependence on the cross-section of samples, which is consistent with Ref. 17. However, detailed investigation on size-dependent optical dispersion and mode competition is still in progress.

In summary, this work demonstrates remarkable effects of nanoribbon ends in Raman scattering. We have studied the polarized Raman properties of V_2O_5 using confocal microscopy. Detailed polarized optical properties analysis indicated that the polar scattering patterns are mainly governed by bulk Raman tensors at the body. While at the tip of the sample, the effective waveguides and tip-enhanced outcoupling would be directly related to the direction of phonon scattering. This gives rise to a pronounced Raman intensity contrast along the sample for certain configuration. The anomalous behavior is expected to be a general effect in other one-dimension nanostructures and demonstrates prospects of the tip effect on optoelectronic nanodevices.

The authors gratefully acknowledge Dr. Qihua Xiong for his beneficial discussions and thank Miss Christina Pang for her helpful comments on this manuscript.

[1] D. J. Sirbuly, M. Law, P. Pauzauskie, H. Q. Yan, A. V. Maslov, K. Knutsen, C. Z. Ning, R. J. Saykally, and P. D. Yang, Proc. Natl. Acad. Sci. U.S.A. **102**, 7800 (2005); F. Qian, Y. Li, S. Gradecak, H. G. Park, Y. J. Dong, Y. Ding, Z. L. Wang, and C. M. Lieber, Nature Mater. **7**, 701 (2008).
[2] B. Yan, L. Liao, Y. M. You, X. J. Xu, Z. Zheng, Z. X. Shen, J. Ma, L. M. Tong, and T. Yu, Adv. Mater. **21**, 2436 (2009).
[3] J. F. Wang, M. S. Gudiksen, X. F. Duan, Y. Cui, and C. M. Lieber, Science **293**, 1455 (2001); H. Pettersson, J. Tragardh, A. I. Persson, L. Landin, D. Hessman, and L. Samuelson, Nano Lett. **6**, 229 (2006); T. Yu, X. Zhao, Z. X. Shen, Y. H. Wu, and W. H. Su, J. Cryst. Growth **268**, 590 (2004).
[4] H. E. Ruda and A. Shik, Phys. Rev. B **72**, 115308 (2005).
[5] L. Y. Cao, B. Nabet, and J. E. Spanier, Phys. Rev. Lett. **96**, 157402 (2006).
[6] Q. Xiong, G. Chen, H. R. Gutierrez, and P. C. Eklund, Appl. Phys. A: Mater. Sci. Process. **85**, 299 (2006).
[7] J. C. Johnson, H. Q. Yan, P. D. Yang, and R. J. Saykally, J. Phys. Chem. B **107**, 8816 (2003); L. K. van Vugt, S. Rühle, and D. Vanmaekelbergh, Nano Lett. **6**, 2707 (2006); G. Chen, J. Wu, Q. J. Lu, H. R. H. Gutierrez, Q. Xiong, M. E. Pellen, J. S. Petko, D. H. Werner, and P. C. Eklund, Nano Lett. **8**, 1341 (2008); V. G. Bordo, Phys. Rev. B **78**, 085318 (2008); S. J. Lee, J. M. Baik, and M. Moskovits, Nano Lett. **8**, 3244 (2008); L. K. van Vugt, S. Rühle, P. Ravindran, H. C. Gerritsen, L. Kuipers, and D. Vanmaekelbergh, Phys. Rev. Lett. **97**, 147401 (2006).
[8] D. O'Carroll, I. Lieberwirth, and G. Redmond, Nat. Nanotechnol. **2**, 180 (2007).
[9] P. J. Pauzauskie, D. Talaga, K. Seo, P. D. Yang, and F. Lagugne-Labarthet, J. Am. Chem. Soc. **127**, 17146 (2005); C.-T. Chien, M.-C. Wu, C.-W. Chen, H.-H. Yang, J.-J. Wu, W.-F. Su, C.-S. Lin, and Y.-F. Chen, Appl. Phys. Lett. **92**, 223102 (2008).
[10] Z. Zheng, B. Yan, J. Zhang, Y. You, C. T. Lim, Z. Shen, and T. Yu, Adv. Mater. **20**, 352 (2008); B. Yan, Z. Zheng, J. X. Zhang, H. Gong, Z. X. Shen, W. Huang, and T. Yu, J. Phys. Chem. C **113**, 20259 (2009).
[11] See supplementary material at http://dx.doi.org/10.1063/1.3323090 for experimental details and Raman tensor analysis.
[12] J. Fréchette and C. Carraro, J. Am. Chem. Soc. **128**, 14774 (2006).
[13] V. Poborchii, T. Tada, and T. Kanayama, Appl. Phys. Lett. **94**, 131907 (2009).
[14] L. Cao, L. Laim, P. D. Valenzuela, B. Nabet, and J. E. Spanier, J. Raman Spectrosc. **38**, 697 (2007).
[15] D. O'Carroll and G. Redmond, Physica E (Amsterdam) **40**, 2468 (2008); D. J. Sirbuly, M. Law, H. Q. Yan, and P. D. Yang, J. Phys. Chem. B **109**, 15190 (2005).
[16] Y. Fedutik, V. Temnov, U. Woggon, E. Ustinovich, and M. Artemyev, J. Am. Chem. Soc. **129**, 14939 (2007).
[17] J. Fréchette and C. Carraro, Phys. Rev. B **74**, 161404 (2006).